

Sputtering of ice grains and icy satellites in Saturn's inner magnetosphere

R.E. Johnson^{a,b,*}, M. Famá^a, M. Liu^a, R.A. Baragiola^a, E.C. Sittler Jr.^c, H.T. Smith^d

^aUniversity of Virginia, Charlottesville, VA 22904, USA

^bDepartment of Physics, NYU, New York, NY 10003, USA

^cGoddard Space Flight Center, Greenbelt, MD, USA

^dApplied Physics Laboratory, Johns Hopkins University, Laurel, MD, USA

Received 3 February 2008; received in revised form 21 March 2008; accepted 14 April 2008

Available online 22 April 2008

Abstract

Icy grains and satellites orbiting in Saturn's magnetosphere are immersed in a plasma that sputters their surfaces. This limits the lifetime of the E-ring grains and ejects neutrals that orbit Saturn until they are ionized and populate its magnetosphere. Here we re-evaluate the sputtering rate of ice in Saturn's inner magnetosphere using the recent Cassini data on the plasma ion density, temperature and composition [Sittler Jr., E.C., et al., 2007a. Ion and neutral sources and sinks within Saturn's inner magnetosphere: Cassini results. *Planet. Space Sci.* 56, 3–18.] and a recent summary of the relevant sputtering data for ice [Famá, M., Shi, J., Baragiola, R.A., 2008. Sputtering of ice by low-energy ions. *Surf. Sci.* 602, 156–161.]. Although the energetic (>10 keV) ion component at Saturn is much smaller than was assumed to be the case after Voyager [Jurac, S., Johnson, R.E., Richardson, J.D., Paranicas, C., 2001a. Satellite sputtering in Saturn's magnetosphere. *Planet. Space Sci.* 49, 319–326; Jurac, S., Johnson, R.E., Richardson, J.D., 2001b. Saturn's E ring and production of the neutral torus. *Icarus* 149, 384–396.], we show that the sputtering rates are sensitive to the temperature of the thermal plasma and are still robust, so that sputtering likely determines the lifetime of the grains in Saturn's tenuous E-ring.

© 2008 Elsevier Ltd. All rights reserved.

Keywords: Sputtering; Saturn; Icy; Magnetosphere

1. Introduction

The sputtering of water ice is of interest in the outer solar system where icy bodies are exposed to energetic ions trapped in the magnetospheres of the giant planets. Sputtering, along with out-gassing, is responsible for populating the magnetospheres with neutrals which orbit Saturn, often referred to as a neutral cloud or, if they are long-lived, a neutral torus. Atoms and molecules in these clouds are eventually ionized by the solar UV photons or the local plasma producing ions that are picked-up and accelerated in the planet's rotating magnetosphere. These ions are trapped in the magnetosphere until they are either transported outward by plasma processes and escape or are

neutralized by charge exchange or electron recombination. Therefore, there is an interesting but complex feedback process between the production and loss of neutrals and the production and loss of ions in a planet's magnetosphere (e.g., Johnson, 1990).

In Saturn's magnetosphere the out-gassing from the fractured south polar region of Enceladus, as well as sputtering of icy bodies and ice grains, are sources of the extended neutral atmosphere of water molecules and their dissociation products observed by the Hubble Space Telescope (HST) (Shemansky et al., 1993; Richardson et al., 1998; Jurac et al., 2002; Jurac and Richardson, 2005); and by the instruments on Cassini (Esposito et al., 2005; Waite et al., 2006; Johnson et al., 2006). Before the discovery of active plumes of gas and dust from the south polar region of Enceladus, sputtering from icy satellites and small ice grains by magnetospheric ions was suggested to be the principal candidate for explaining the population

*Corresponding author at: University of Virginia, Charlottesville, VA 22904, USA. Tel.: +1 434 924 3244; fax: +1 434 924 1353.

E-mail address: rej@virginia.edu (R.E. Johnson).

of this atmosphere (Johnson et al., 1989; Jurac et al., 2001a, b). However, preliminary estimates of the sputter flux (Shi et al., 1995; Jurac et al., 2001b) gave results for the sputtering rate that were at least one order magnitude below the production rate of water molecules required to populate the OH cloud observed by HST unless there was a large population of very small undetected grains (Jurac et al., 2002). Sputtering was still expected to be an important process for limiting the grain lifetimes of the E-ring grains and was an important source of neutrals outside the orbit of Dione (Jurac et al., 2002; Jurac and Richardson, 2005).

The recent observations of plasma in Saturn's inner magnetosphere ($< \sim 10 R_S$, where $1 R_S$ is a Saturn radius) by instruments on the Cassini spacecraft reveal that the ion composition is mainly protons and water group ions (O^+ , OH^+ , H_2O^+ , H_3O^+) with energies peaking at hundreds eV (Young et al., 2005; Sittler et al., 2005, 2007a; Tokar et al., 2006). Famá et al. (2008) recently obtained new sputtering data for water ice, which they combined with earlier measurements to produce a semi-empirical model for the sputtering yield (number of molecules ejected per ion incident) that is applicable in this energy region. These data are used here along with recent measurements of the ion densities and temperatures from the Cassini Plasma Spectrometer (CAPS) (Sittler et al., 2006, 2007a, b) to give new estimates for the sputtering rates in Saturn's magnetosphere.

2. Saturnian plasma

Since heavy ions with energies $> \sim 10$ keV were found to be the dominant sputtering agent for icy materials in the Jovian magnetosphere (e.g., Johnson, 1990; Cooper et al., 2001), this was initially assumed to be the case also at

Saturn (Shi et al., 1995; Jurac et al., 2001b). Cassini data showed that the presence of a relatively dense and extended population of neutrals suppresses the very energetic ions in the region inside of $10 R_S$ (Paranicas et al., 2008). The energetic electron population, which at Europa contributes to forming the O_2 atmosphere, is also considerably reduced in Saturn's inner magnetosphere ($< \sim 15 R_S$; Rymer et al., 2007; Paranicas et al., 2007). Therefore, the erosion of E-ring grains, the erosion of the dust halo at Rhea (Jones et al., 2008) and sputtering of satellite surfaces inside the orbit of Rhea is likely dominated by ions with energies < 10 keV, opposite to what has been assumed in earlier work. In the model below the O_2 and H_2 ejected due to decomposition is included with water molecule ejection giving the total sputtering rate in equivalent H_2O ejected. If one is only interested only in the production of O_2 , for instance, then the energy deposited by energetic electrons and ions must be included and compared with the temperature dependent component of the yield used below. This will be described in subsequent work.

Figs. 1a and b give the ion densities and temperatures in Saturn's inner magnetosphere as measured by the CAPS instrument (Sittler et al., 2007a, b). These are given in Saturn's equatorial plane as a function of radial distance from Saturn from 3.5 to $10 R_S$ ($R_S \approx 60,268$ km), a region in which many of the icy satellites and the E-ring grains orbit. The plasma is primarily produced from the water plumes on Enceladus and the densities are given for H^+ and for water-like species summed together as W^+ (O^+ , OH^+ , H_2O^+ , and H_3O^+). The composition of this component varies with radial distance, with H_3O^+ being an important contribution near Enceladus ($\sim 4 R_S$) (Tokar et al., 2006) and O^+ becoming dominant by $10 R_S$ near the orbit of Rhea (Sittler et al., 2007a). Although a single temperature is given at each value of R , the plasma ion velocity

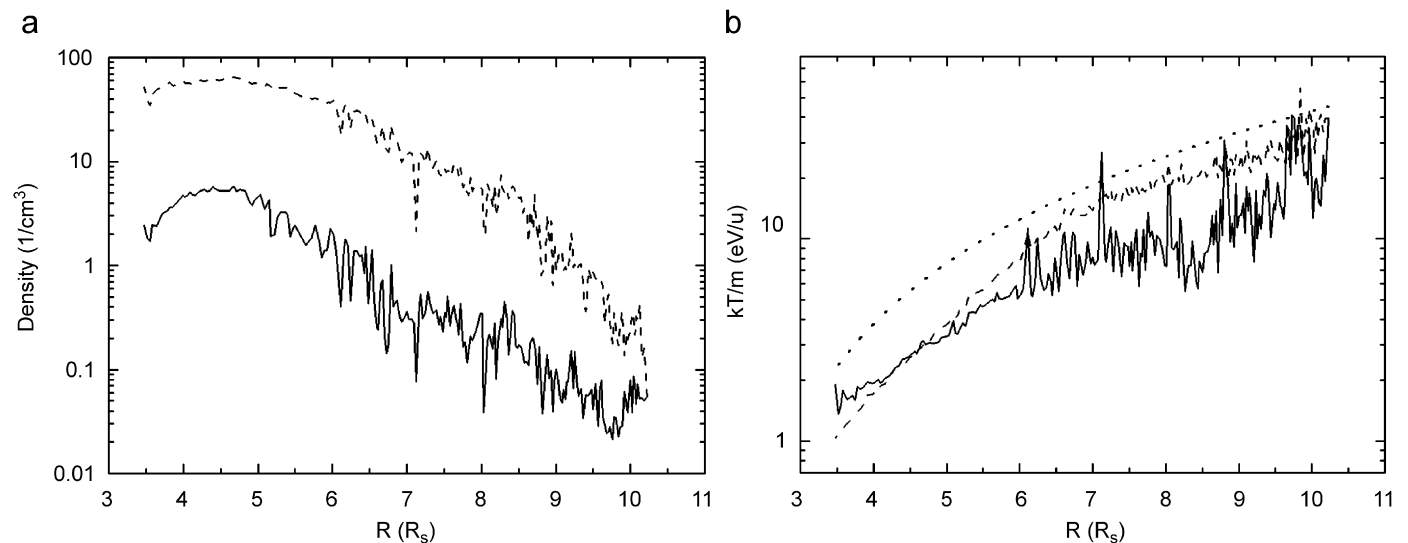


Fig. 1. (a) The ion densities in Saturn's inner magnetosphere as measured by the CAPS instrument. The densities are given for H^+ (solid line) and water-like species summed together as W^+ (O^+ , OH^+ , H_2O^+ , and H_3O^+). (b) The ion temperatures for H^+ (solid) and W^+ (dashed) measured relative to the plasma flow speed. The dotted line in (b) corresponds to the energy associated with the flow past a grain or satellite orbiting in Saturn's magnetosphere [approximately the gyro-energy that ions get when they are picked up by the field: $m_i(\vec{v}_{co} - \vec{v}_o)^2/2$].

distributions are not isotropic. The velocity distribution is divided into components perpendicular to the local magnetic field, T_{\perp} , and parallel, T_{\parallel} , with $T = (2T_{\perp} + T_{\parallel})/3$. The relative contribution of these to the total flux differs between ions and varies slowly with R . Sittler et al. (2007a) suggest $T_{\parallel}/T_{\perp} \sim 0.5$ for protons and $T_{\parallel}/T_{\perp} \sim 0.2$ for W^+ at the magnetic equator. Such ratios indicate that the ion lifetimes are too short for the temperature to isotropize (Tokar et al., 2008). Since these temperatures are measured relative to the plasma flow speed, we also show in Fig. 1b the energy associated with the flow past a grain or satellite orbiting in Saturn's magnetosphere. That is, the ions obtain gyro-motion on pick-up given as $m_i(\vec{v}_{co} - \vec{v}_o)^2/2$, where \vec{v}_{co} is the tangential velocity of rotation of the magnetic field which confines the plasma, and \vec{v}_o is the orbital speed of the body. Since Saturn's field is closely aligned with its spin axis, for bodies in circular orbit these velocities have, roughly, the same direction; using Saturn's rotational speed and gravity at its equator, the speeds are $v_{co} \approx 9.87R(R_S) \text{ km s}^{-1}$ and $v_o \approx 25.1/[R(R_S)]^{1/2} \text{ km s}^{-1}$, where R is the radial distance in R_S . These ion speeds and densities are used below to calculate sputtering rates.

3. Calculation of sputtering flux

Sputtering can occur in ice by direct momentum transfer from the projectile to a target atom, by long-lived repulsive electronic excitations which lead to atomic or molecular motion, or by chemical reactions (e.g., Johnson, 1990, 1996). Momentum transfer sputtering, often called elastic nuclear, collision cascade or knock-on sputtering, is well understood in atomic solids. A detailed theoretical, computational and experimental compilation is found in Behrisch and Eckstein (2007). However, the sputtering of molecular insulators by either momentum transfer events or electronic processes is not well understood since molecular dissociation and chemistry play a critical role so that the erosion rates depend on the surface temperature.

For an ion penetrating ice, the sputtering yield Y , the number of molecules ejected per ion incident, has been shown to depend on the energy deposited by the incident ion per unit path length in the material, (dE/dx) , often called the stopping power. The yield due to momentum transfer to target atoms was found to depend nearly linearly on $(dE/dx)_n$, the elastic nuclear component of (dE/dx) (Famá et al., 2008), which is well known for atomic materials but was debated for icy molecular solids. Brown et al. (1980) noted the importance of electronic processes for sputtering ice and showed this component varied roughly as $(dE/dx)_e^2$, where the subscript implies the electronic component of the energy deposited. These dependences have since been shown to apply over a broad range of ion energies and types for ice temperatures $< \sim 120 \text{ K}$ (Brown et al., 1982; Johnson, 1996; Baragiola et al., 2003; Famá et al., 2008). Since dE/dx depends on the molecular density of the material, n , it is typically written as $dE/dx = nS$, where S is called the stopping cross section.

In addition, as the angle of incidence relative to the surface normal increases, the energy is deposited closer to the surface increasing the yield (e.g., Johnson, 1990; Famá et al., 2008). Finally, due to the dissociations produced by both the elastic nuclear collisions and electronic excitations, chemistry occurs with an activation energy E_a . Therefore, the yields are modified by $[1 + A \exp(-E_a/kT)]$ where T is the surface temperature and E_a and A are determined empirically (Johnson, 1990; Famá et al., 2008). The second term determines the contribution to the yield due to decomposition of ice producing O_2 and H_2 (e.g., Reimann et al., 1984; Johnson and Quickenden, 1997; Teolis et al., 2005).

Based on the above discussion, the yield is linear in $S_n(E_i)$, the elastic nuclear stopping cross section, but quadratic in $S_e(E_i)$, the electronic stopping cross section where E_i is the incident ion energy. Therefore, it can be written as (e.g., Johnson, 1990; Famá et al., 2008):

$$Y_{H_2O}(E_i, \theta) = \frac{[C'(m_i)S_n + \eta(Z_i)S_e^2][1 + A e^{-E_a/kT}]}{[\cos \theta_i]^{(1+x)}}; \quad (1)$$

$$E_i \gg E_t,$$

where the empirical constants C' , η , A , E_a and x are given below. The terms in the second bracket give the enhancement due to surface temperature, the terms in the third bracket the enhancement due to incident angle, θ_i (Johnson, 1989), and E_t is a threshold energy below which sputtering is improbable and the yield is essentially zero. For sputtering of water ice by a singly charged ion of mass m_i and nuclear charge Z_i at speeds below the maximum in S_e , Famá et al. (2008) used $E_a = 0.06 \text{ eV}$; $A = 220$; $C'(m_i) \approx 0.0332[1 + 4.9 \exp(-0.870m_i) + 1.48 \exp(-0.105m_i)] \text{ (eV } \text{Å}^2)^{-1}$; $x \approx 0.3 + 0.13 \ln(m_i)$; $\eta(Z_i) \approx 0.0004939 + 0.0029613 \sin^2[2.72923(Z_i - 1)^{0.31812}] \text{ (eV } \text{Å}^2)^{-2}$ with m_i in atomic mass units. The resulting yields compare reasonably well with earlier estimates (e.g., Johnson, 1990, 1996). Since the temperatures are less than 100 K for the icy surface in the Saturnian system, $T = 80 \text{ K}$ is used below. The S_n and S_e can be obtained from the freeware program SRIM (Ziegler et al., 1985; <http://www.srim.org/>) for stopping of ions in water. Alternatively, an analytic expressions based on a scaled energy variable was given by Famá et al. (2008). The yield expression was tested experimentally down to $\sim 100 \text{ eV}$ with some simulations for slightly lower energies. Because these are mass loss measurements, given here as equivalent H_2O molecules ejected per ion incident, the implantation of the incident H^+ or O^+ is accounted for in the net yield, as is the loss due to production of O_2 and H_2 . Threshold energies have been estimated for a variety of solids (Behrisch and Eckstein, 2007) but not for ice. Based on the incident ion to target molecule mass ratio, a value of ~ 10 times the sublimation energy, or $\sim 5 \text{ eV}$ is appropriate for protons at normal incidence and decreases slightly with increasing angle of incidence. Since the threshold region is steep we use a simple cut-off, and set the yield to zero below 5 eV . For O^+ , the 5 eV threshold energy has no effect on the

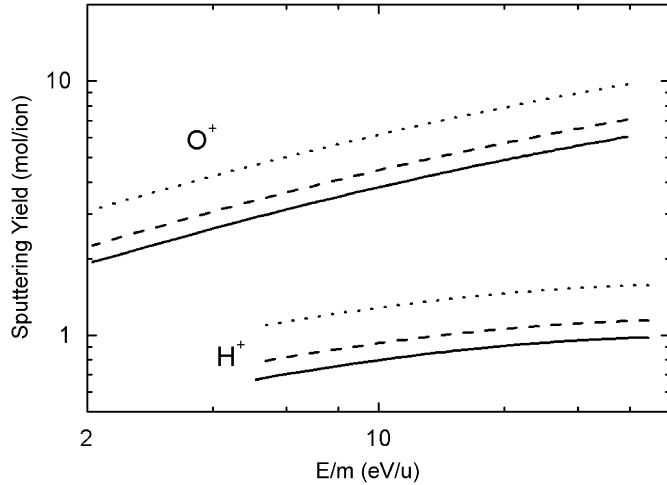


Fig. 2. Sputtering yield of ice for H^+ and O^+ at normal incidence vs. ion energy, E_i ($eV amu^{-1}$): T (solid, 80 K); (dashed, 100 K); (dotted, 120 K); $E_i = 5 eV$ (the region near E_i has not been studied experimentally for ice). These yields are roughly consistent with those in Fig. 3.22b in Johnson (1990) and Fig. 2 in Johnson (1996) at the higher energies shown but are larger at the lower energies.

calculated results. Fig. 2 shows results for the sputtering yield of ice, according to Eq. (1), for H^+ and O^+ at normal incidence for $E_i > 5 eV$ and $T = 80, 100, \text{ and } 120 K$.

Using the ion density, n_i , and velocity distribution, $f(\vec{v})$, along with the sputtering yield above, $Y_{H_2O}(E_i, \theta)$, the surface-averaged sputter flux can be written (e.g., Johnson, 1990; Cooper et al., 2001):

$$\Phi_{\text{sputtering}} = \iint Y_{H_2O}(E_i, \theta) [-\hat{n}(\vec{u} + \vec{v})] n_i f(\vec{v}) d^3v \frac{d\Omega_s}{4\pi}. \quad (2)$$

Here \vec{u} is the average flow velocity of the ions relative to the body and \hat{n} is the local surface normal. The flux is averaged over the body by integrating $d\Omega_s$ over the direction of the surface normal which varies with the position on the body. The flow speed at a grain or satellite orbiting Saturn is $\vec{u} = \vec{v}_{co} - \vec{v}_o$. Replacing $Y_{H_2O}(E_i, \theta)$ by one give the incident flux averaged over the surface, Φ_i . The average yield per incident ion, which is useful if the plasma density estimates change, is then written as $\bar{Y} = \Phi_{\text{sputtering}}/\Phi_i$. The sputter flux can also be given as a surface erosion rate by dividing by the molecular number density of ice, n_{ice} and the surface erosion speed is $\Phi_{\text{sputtering}}/n_{ice}$ in depth per unit time.

The local sputter flux and yield can be calculated at any point on the surface by not averaging over the orientation of the surface normal. However, here we use Eqs. (2) and (3) which are averages over the body, giving a result that can be used in a number of circumstances. Initially we ignore surface porosity or roughness. If we assume an approximately spherical body, the integrals simplify. Holding $\vec{v}_i = \vec{u} + \vec{v}$ fixed, the average over a spherical surface is the same for each \vec{v}_i . Writing $Y(E_i, \theta_i) = Y(E_i)g(\cos \theta_i)$ then the average over $d\Omega_s/4\pi$ is $\bar{g} = \int_{\cos \theta_m}^2 g(\cos \theta_i) 2 \cos \theta_i d \cos \theta_i$, where $\theta_i = \theta_m$ is the

incident angle beyond which the yield rapidly decreases due to ion scattering at grazing incidence. Here that angle is used as a cut-off. Using the angular dependence given in Eq. (1), $g(\cos \theta_i) \approx 1/\cos^{1+x} \theta_i$, the integral becomes $\bar{g} \approx (2/(1-x))[1 - \cos^{1-x} \theta_m]$. Therefore, we can write the sputter flux averaged over a spherical surface,

$$\Phi_{\text{sputtering}} = \bar{g} \frac{n_i}{4} \iint Y(E_i, 0) |\vec{u} + \vec{v}| f(\vec{v}) d^3v, \quad (3)$$

with $E_i = m_i |\vec{u} + \vec{v}|^2/2$. This applies to a grain, but for a rough or porous satellite regolith a correction is required since sputtered molecules can re-condense on surface of a nearby grain prior to escaping from the regolith (Cassidy and Johnson, 2005).

We calculate $\Phi_{\text{sputtering}}$ for two cases. First, since the ion temperatures are not high we ignore the velocity distribution $f(\vec{v})$ and assume that $v = 0$ so that $E_i = (1/2)m_i u^2$ and,

$$\Phi_{\text{sputtering}} = \bar{g} \frac{u n_i}{4} Y(E_i, 0). \quad (4)$$

Therefore, on the average, ions flow onto the object at a speed, u , equal to the co-rotation speed minus the orbital speed: $u = |\vec{v}_{co} - \vec{v}_o| = 18.4[(R/R_x) - (R_x/R)^{1/2}] km s^{-1}$ with $R_x = 1.86 R_s$. We compare this to a calculation in which we use T_{\parallel} and T_{\perp} to get a product of Maxwellian distributions in the form $f(\vec{v}) d^3v = f(v_{\parallel})f(v_{\perp}) dv_{\parallel} d^2v_{\perp}$. For the ion temperature $T_i = (2/3)T_{\perp} + (1/3)T_{\parallel}$, with $T_{\perp} = 2 T_{\parallel}$ for the protons and $T_{\perp} = 5 T_{\parallel}$ for W^+ .

4. Results

Ion density and temperature data from Figs. 1a and b are used to calculate the globally averaged sputter flux shown in Fig. 3, by first assuming only plasma flow onto an icy body and assuming the W^+ ions are well represented by O^+ . Then, we include the ion thermal motion. Not surprisingly,

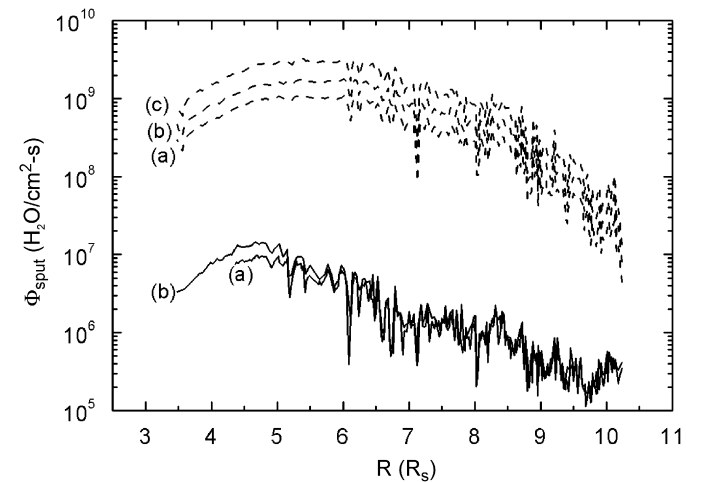


Fig. 3. Sputtering rate of water molecules according to Eq. (3) and including the threshold discussed: solid H^+ , dashed W^+ : (a) ion temperatures ignored ($W^+ \rightarrow O^+$); note threshold effect for H^+ ; (b) includes ion temperatures ($W^+ \rightarrow O^+$); (c) includes ion temperatures ($W^+ \rightarrow H_2O^+$).

this inclusion increases significantly the sputter flux, due to the more energetic ions in the tail of the distribution. When considering the flux tube content, Sittler et al. (2007a) showed that the mean ion mass was consistent with mass 18. Therefore, for comparison we also repeat the calculation assuming all W^+ are H_2O^+ ; that is, $S \approx S_O + 2S_H$ in Eq. (1) for both the nuclear elastic and electronic stopping powers producing a further increase in the sputter flux. As better measurements of the ion composition and energy distributions become available, the expressions here can be used to obtain more detailed estimates of the sputtering rate.

5. Results and conclusions

The net sputter flux of icy surfaces in the Saturnian system is primarily due to the water ion plasma. These yield are not negligible even though the energetic ion component of the plasma in Saturn's inner magnetosphere differs from that in the Jovian magnetosphere, both in the absence of a significant 'hot' component (> 10 keV) and in the absence of energetic sulfur ions which sputter very efficiently (e.g., Cooper et al., 2001). It is also seen that for the sputtering of the icy satellites in the Saturnian system, where the $(v_{co} - v_o)$ is much smaller than it is for the icy jovian satellites, the yield is sensitive, not surprisingly, to the ion temperature. Therefore, accurate ion temperatures, as well as ion composition are important in determining satellite and grain erosion rates. Here we have used recently available spacecraft and laboratory data, as described above, to determine sputtering yields that can be used to calculate the lifetime of E-ring grains and the sputter contribution to the neutral torus. Inside about of $6 R_S$ the small negative grain charge (Jurac et al., 1995) can slightly increase the ion impact energy and the corrections for sputtering of very small grains can be included (Jurac et al., 1998, 2001b).

The rates presented here are for the total surface loss given in equivalent H_2O , some of which is due to ice decomposition producing O_2 and H_2 . This small component is contained in the temperature dependent term ($\sim 3\%$ at 80 K). To accurately estimate the total O_2 source rate, the decomposition due to the energy deposited by the energetic ions and electrons needs to be included (e.g., Johnson et al., 2003).

Noting that the plasma is predominantly molecular in the inner magnetosphere, an average erosion rate $\sim 10^9 \text{ cm}^{-2} \text{ s}^{-1}$ is applicable, so that a grain with a $1 \mu\text{m}$ diameter would survive ~ 50 years, which is not very different from earlier estimates (Jurac et al., 2001b). In addition, although sputtering is a small contributor to the total neutral supply rate and the escape from Enceladus is dominated by the plumes at the south pole ($\sim 10^{28} \text{ H}_2\text{O s}^{-1}$), Burger et al. (2007) showed that the Cassini INMS observations of the spatial morphology of the local Enceladus cloud appear to require a small, additional 'global' contribution of $\sim 8 \times 10^{25} \text{ H}_2\text{O s}^{-1}$ (see also, Waite et al., 2006). Using the globally averaged sputter flux for incident H_2O^+ in Fig. 3 ($\sim 2 \times 10^9 \text{ cm}^{-2} \text{ s}^{-1}$) and the area of Enceladus

($\sim 8 \times 10^{15} \text{ cm}^2$), a source of the order of that required in Burger et al. (2007) is obtained, allowing for the considerable uncertainties. Similarly, we note that the sputter rates near Tethys and Dione are robust and the neutral source rate due to sputtering of the icy dust halo around Rhea (Jones et al., 2008) can now be estimated. Although the mass loading close to Rhea appears to be small (Khurana et al., 2008), the plasma has access to the surface and dust particles so that the sputter contribution to the local neutral torus is not negligible.

The net sputtering rates given here were calculated assuming a laboratory-like surface. This is appropriate for the sputtering of grains and the dust particles in Rhea's halo. However, the icy satellites are known to have rough and porous regoliths, which result in a reduction of the sputter flux if the ejected molecules stick to neighbors (Cassidy and Johnson, 2005; Jurac et al., 2001a). At Enceladus this reduction is likely more than compensated for by the fact that its surface is continuously coated with fresh, fluffy deposits from its plumes and such deposits of small grains can have higher sputtering yields (e.g., Johnson, 1990). Therefore, plasma ion sputtering remains an important consideration in the distribution of neutrals and in the erosion of icy surfaces throughout Saturn's inner magnetosphere.

Acknowledgments

We acknowledge support from NASA's Cassini project via SwRI and the CAPS instrument. REJ also acknowledges support from NASA's Planetary Geology and Geophysics Program.

References

- Baragiola, R.A., Vidal, R.A., Svendsen, W., Schou, J., Shi, M., Bahr, D.A., Atteberry, C.L., 2003. Sputtering of water ice. Nucl. Instrum. Methods Phys. Res. B 209, 294–303.
- Behrisch, R., Eckstein, W., 2007. Sputtering by Particle Bombardment. Experiments and Computer Calculations from Threshold to MeV Energies. Springer, Berlin.
- Brown, W.L., Augustyniak, W.M., Lanzerotti, L.J., Johnson, R.E., Evatt, R., 1980. Linear and nonlinear processes in the erosion of H_2O ice by fast light ions. Phys. Rev. Lett. 45 (20), 1632–1635.
- Brown, W.L., Augustyniak, W.M., Simmons, E., Marcantonio, K.J., Lanzerotti, L.J., Johnson, R.E., Boring, J.W., Reimann, C.T., Foti, G., Pirronello, V., 1982. Erosion and molecular formation in condensed gas films by electronic energy loss of fast ions. Nucl. Instrum. Methods 198, 1.
- Burger, M.H., Sittler Jr., E.C., Johnson, R.E., Smith, H.T., Tucker, O.J., Shematovich, V.I., 2007. Understanding the escape of water from Enceladus. J. Geophys. Res. 112, A06219.
- Cassidy, T.A., Johnson, R.E., 2005. Monte Carlo model of sputtering and other ejection processes within a regolith. Icarus 176, 499–507.
- Cooper, J.F., Johnson, R.E., Mauk, B.H., Garrett, H.B., Gehrels, N., 2001. Energetic ion and electron irradiation of the Icy Galilean satellites. Icarus 149, 133–159.
- Esposito, L.W., Colwell, J.E., Larsen, K., et al., 2005. Ultraviolet imaging spectroscopy shows an active Saturnian system. Science 307, 1251.
- Famá, M., Shi, J., Baragiola, R.A., 2008. Sputtering of ice by low-energy ions. Surf. Sci. 602, 156–161.

- Johnson, R.E., 1989. Electronic sputtering: angular and charge-state dependence of the yield via superposition. *J. Phys. C* 2, 251–257.
- Johnson, R.E., 1990. *Energetic Charged-particle Interactions with Atmospheres and Surfaces*. Springer, New York.
- Johnson, R.E., 1996. Sputtering of ices in the outer solar system. *Rev. Mod. Phys.* 68, 305–312.
- Johnson, R.E., Quickenden, T.I., 1997. Photolysis and radiolysis of water ice on outer solar system bodies. *J. Geophys. Res. E* 102, 10,985–10,996.
- Johnson, R.E., Pospieszalska, M.K., Sittler, E.C., Cheng, A.F., Lanzerotti, L.J., Sieveka, E.M., 1989. The neutral cloud and heavy ion inner torus at Saturn. *Icarus* 77, 311–329.
- Johnson, R.E., Quickenden, T.I., Cooper, P.D., McKinley, A.J., Freeman, C., 2003. The production of oxidants in Europa's surface. *Astrobiology* 3, 823–850.
- Johnson, R.E., Smith, H.T., Tucker, O.J., Liu, M., Tokar, R., 2006. The Enceladus and OH tori at Saturn. *Astrophys. J. Lett.* 644, L137–L139.
- Jones, G.H., et al., 2008. The dust halo of Saturn's largest icy moon, Rhea. *Science* 319, 1380–1384.
- Jurac, S., Richardson, J.D., 2005. A self-consistent model of plasma and neutrals at Saturn: neutral cloud morphology. *J. Geophys. Res.* 110, A09220.
- Jurac, S., Baragiola, R.A., Johnson, R.E., Sittler Jr., E.C., 1995. Charging of ice grains by low energy plasmas: applications to Saturn's E-ring. *J. Geophys. Res.* 100, 14,821–14,831.
- Jurac, S., Johnson, R.E., Donn, B., 1998. Monte Carlo calculation of enhancement in the sputtering of small grains. *Astrophys. J. Lett.* 503, 247–252.
- Jurac, S., Johnson, R.E., Richardson, J.D., Paranicas, C., 2001a. Satellite sputtering in Saturn's magnetosphere. *Planet. Space Sci.* 49, 319–326.
- Jurac, S., Johnson, R.E., Richardson, J.D., 2001b. Saturn's E ring and production of the neutral torus. *Icarus* 149, 384–396.
- Jurac, S., McGrath, M.A., Johnson, R.E., Richardson, J.D., Vasyliunas, V.M., Eviatar, A., 2002. Saturn: search for a missing water source. *Geophys. Res. Lett.* 29 (24), 2172.
- Khurana, K.K., Russell, C.T., Dougherty, M.K., 2008. Magnetic portraits of Tethys and Rhea. *Icarus* 193, 465–474.
- Paranicas, C., Mitchell, D.G., Roelof, E.C., Mauk, B.H., Krimigis, S.M., Brandt, P.C., Kusterer, M., Turner, F.S., Vandegriff, J., Krupp, N., 2007. Energetic electrons injected into Saturn's neutral gas cloud. *Geophys. Res. Lett.* 34, L02109.
- Paranicas, C., Mitchell, D.G., Krimigis, S.M., Hamilton, D.C., Roussos, E., Krupp, N., Jones, G.H., Johnson, R.E., Cooper, J.F., Armstrong, T.P., 2008. Sources and losses of energetic protons in Saturn's magnetosphere. *Icarus*, in press.
- Reimann, C.T., Boring, J.W., Johnson, R.E., Garrett, J.W., Farmer, K.R., Brown, W.L., 1984. Ion-induced molecular ejection from D₂O ice. *Surf. Sci.* 147, 227.
- Richardson, J.D., Eviatar, A., McGrath, M.A., Vasyliunas, V.M., 1998. OH in Saturn's magnetosphere: observations and implications. *J. Geophys. Res.* 103, 20245–20255.
- Rymer, A.M., Mauk, B.H., Hill, T.W., Paranicas, C., Andre, N., Sittler, E.C., Mitchell, D.G., Smith, H.T., Johnson, R.E., Coates, A.J., Young, D.T., Bolton, S.J., Thomsen, M.F., Dougherty, M.K., 2007. Electron sources in Saturn's magnetosphere. *J. Geophys. Res.* 112, A02201.
- Shemansky, D.E., Matheson, P., Hall, D.T., Hu, H.-Y., Tripp, T.M., 1993. Detection of the hydroxyl radical in the Saturn magnetosphere. *Nature* 363, 329–331.
- Shi, M., Baragiola, R.A., Grosjean, D.E., Johnson, R.E., Jurac, S., Schou, J., 1995. Sputtering of water ice surfaces and the production of extended neutral atmospheres. *J. Geophys. Res.* 100, 26,387–26,395.
- Sittler Jr., E.C., et al., 2005. Preliminary results on Saturn's inner plasmasphere as observed by Cassini: comparisons with Voyager. *Geophys. Res. Lett.* 32 (14), L14S04.
- Sittler Jr., E.C., et al., 2006. Cassini observations of Saturn's inner plasmasphere: Saturn orbit insertion results. *Planet. Space Sci.* 54, 1197–1210.
- Sittler Jr., E.C., et al., 2007a. Ion and neutral sources and sinks within Saturn's inner magnetosphere: Cassini results. *Planet. Space Sci.* 56, 3–18.
- Sittler Jr., E.C., et al., 2007b. Erratum to “Cassini observations of Saturn's inner plasmasphere: Saturn orbit insertion results”. *Planet. Space Sci.* 55, 2218–2220.
- Teolis, B.D., Vidal, R.A., Shi, J., Baragiola, R.A., 2005. Mechanisms of O₂ sputtering from water ice by keV ions. *Phys. Rev. B* 72, 245422+9.
- Tokar, R.L., et al., 2006. The interaction of the atmosphere of Enceladus with Saturn's plasma. *Science* 311, 1409.
- Tokar, R.L., Wilson, R.J., Johnson, R.E., Henderson, M.G., Thomas, M.F., Cowee, M.M., Sittler Jr., E.C., Young, D.T., McAndrews, H.J., Smith, H.T., 2008. Cassini detection of water group pick-up ions in Saturn's toroidal atmosphere. *Geophys. Res. Lett.*, under review.
- Waite, J.H., et al., 2006. Cassini ion and neutral mass spectrometer: Enceladus plume composition and structure. *Science* 311, 1419–1422.
- Young, D.T., et al., 2005. Composition and dynamics of plasma in Saturn's magnetosphere. *Science* 307, 1262–1266.
- Ziegler, J.F., Biersack, J.P., Littmark, U., 1985. *The Stopping and Range of Ions in Matter*. Pergamon Press, New York.